

A WEAKLY NONLINEAR ANALYSIS OF ELASTO-PLASTIC-MICROSTRUCTURE MODELS*

LIANJUN AN[†] AND ANTHONY PEIRCE[‡]

Abstract. At certain critical values of the hardening modulus, the governing equations of elasto-plastic flow may lose their hyperbolicity and exhibit two modes of ill-posedness: shear-band and flutter ill-posedness. These modes of ill-posedness are characterized by the uncontrolled growth of modes at infinitely fine scales, which ultimately violates the continuum assumption. In previous work [L. An and A. Peirce, *SIAM J. Appl. Math.*, 54(1994), pp. 708–730], a continuum model accounting for microscale deformations was built. Linear analysis demonstrated the regularizing effect of the microstructure and provided a relationship between the width of the localized instabilities and the microlength scale. In this paper a weakly nonlinear analysis is used to explore the immediate post-critical behavior of the solutions. For both one-dimensional and anti-plane shear models, post-critical deformations in the plastic regions are shown to be governed by the Boussinesq equation (one of the completely integrable PDEs having soliton solutions), which describes the essential coupling between the focusing effect of the nonlinearity and the dispersive effect of the microstructure terms. The soliton solution in the plastic region is patched to the solution in the elastic regions to provide a special solution to the weakly nonlinear system. This solution is used to derive a relation between the width of the shear band and the length scale of the microstructure. A multiple scale analysis of the constant displacement solution is used to reduce the perturbed problem to a nonlinear Schrödinger equation in the amplitude functions—which turn out to be unstable for large time scales. Stability analyses of more complicated special solutions show that the low wave number solutions are unstable even on the fast time scales while the high wave numbers are damped by the dispersive microstructure terms. These theoretical results are corroborated by numerical evidence. This pervasive instability in the strain-softening regime immediately after failure, indicates that the material will rapidly move to a lower residual stress state with well-defined shear bands.

Key words. ill-posed equations, granular materials, shear banding, shear strain softening, loss of hyperbolicity, singular perturbation, solitons

AMS subject classifications. 73H10, 73E99, 35M05

1. Introduction. At certain critical values of the hardening modulus the governing equations of elasto-plastic flow can change type from hyperbolic to elliptic. This change of type within a subdomain results in ill-posedness [11]–[13], [2] which is characterized by uncontrolled growth of the amplitude of plane wave solutions in certain directions. Two modes of instabilities result from the onset of ill-posedness: namely the stationary shear-band instability and the moving flutter instability—which are observed in granular materials such as density waves that occur when sand flows through a hopper [7], and also in the failure modes of brittle rock around deep tabular mining excavations [8].

Since the governing equations are not in conservation form (because of the history dependence of the constitutive relation), it is not possible to derive shock solutions to these equations which account for the instabilities. Linear analysis yields sufficient criteria for the onset of these instabilities. However, the uncontrolled growth of these

* Received by the editors September 14, 1993; accepted for publication (in revised form) March 18, 1994. This research was supported by the National Sciences and Engineering Research Council of Canada.

[†] Department of Applied Mathematics and Statistics, State University of New York at Stony Brook, Stony Brook, New York, 11794.

[‡] Department of Mathematics and Statistics, McMaster University, Hamilton, Ontario, Canada L8S 4K1.

unstable modes does not occur in practice since the generation of arbitrarily fine-scales eventually violates the continuum assumption. To correct the model we have incorporated [4] two types of microstructure: one accounts for inter-granular rotations via Cosserat theory and the other accounts for the formation of microscopic voids by means of a pressure term related to the gradient of the dilation. By linear analysis it is possible to show that the additional higher order microstructure terms, which are dispersive, serve to regularize the solution and inhibit both modes of ill-posedness. It is also possible using matched asymptotics and WKB theory to derive a relation between the thickness of the localization internal layer and the internal length scale implied by the small microstructure terms.

The previous investigations [5] have been restricted to linear analysis. To explore the post-critical behavior of these elasto-plastic-micro (E-P-M) media, nonlinear effects need to be included. In this paper, we carry out a weakly nonlinear analysis of elasto-plastic-micromaterials for simplified stress states. We show that the interaction between the lower order nonlinear terms that change type and the small, higher order, dispersive microstructure terms leads to equations that have a soliton structure locally. In fact, by reformulating the governing equations in terms of displacements, it is possible to reduce the problem to the solution of the Boussinesq equation—one of the completely integrable PDEs exhibiting soliton solutions [1], [9]. The competition of the focusing effect of the nonlinearity (near the critical state) and the spreading effect of the dispersive microstructure terms, leads to a well-posed but growing “jump” profile in which the unstable modes fall within the limits of the continuum assumption.

In §2, we introduce the governing equations and constitutive laws with microstructure. In §3, we analyze a 1-D model—the longitudinal motion of an elasto-plastic bar and a 2-D model—anti-plane shearing. By performing a perturbation expansion near the critical state and retaining second order terms, we obtain a system of nonlinear, history-dependent equations in terms of the displacement gradients. In §4, we demonstrate that the stationary solitary wave solution in the plastic region can be patched to the elastodynamic solution on either side of the localization layer which leads to the desired jump profile. In §5, we use a multiple scales analysis to show that the constant displacement solution in the plastic region (near critical state) is not stable. The instability of other special solutions is also demonstrated. In §6, we provide numerical results which illustrate the analysis presented in this paper. In §7 we summarize the results of this paper and make some concluding comments.

2. The governing equations and constitutive law. In this paper, we consider an elasto-plastic material in which microscale rotational effects (e.g., due to slip between grains) are modeled by a continuum description using Cosserat theory, and microscale dilational effects (e.g., due to microscale voiding) are modeled by introducing a new pressure term into the constitutive relations. The summation convention is assumed unless otherwise specified.

The unknowns consist of the density ρ , velocity v and the Cauchy stress T , subject to the following equations

$$(2.1) \quad \begin{aligned} (a) \quad & \partial_t \rho + \rho \operatorname{div} v = 0, \\ (b) \quad & \rho \partial_t v_j - \partial_i T_{ij} = 0, \end{aligned}$$

which express the conservation of mass and momentum respectively. For simplicity, and because the inclusion of Lagrangian terms does not alter our results in a fundamental way, we use the ordinary derivative ∂_t instead of the material derivative. In fact, we may assume that the deformation rate is small because the deformation is

rate-independent in our model. This assumption allows us to ignore the convective term and to concentrate our analysis on the constitutive nonlinearity which causes the system to change type.

We now provide a brief description of the constitutive law used in this paper. A general derivation of elasto-plastic models can be found in [12], [13], [2] while a description of elasto-plastic models with microstructure is provided in [4]. We decompose the Cauchy stress T into three parts, the symmetric, the antisymmetric and the dispersive pressure

$$T_{ij} = T_{ij}^{(s)} + T_{ij}^{(a)} + p\delta_{ij}$$

and decompose the strain rate V , given by

$$V_{kl} = \frac{1}{2}(\partial_k v_l + \partial_l v_k),$$

into the elastic and plastic parts

$$(2.2) \quad V = V^{(e)} + V^{(p)}.$$

Also we define the deviator and the norm of a tensor $\{A_{ij}\}$ as follows:

$$\text{dev } A = A - \frac{1}{n} \text{tr}(A)I, \quad |A|^2 = \frac{1}{2}A_{ij}A_{ij},$$

where n is the dimension of the spatial variables.

It follows from the linear elasticity theory that

$$(2.3) \quad V_{ij}^{(e)} = C_{ijkl}\partial_t T_{kl}^{(s)},$$

where C is a fourth-order tensor whose inverse E can be expressed through the shear modulus G and Poisson's ratio ν

$$E_{ijkl} = \frac{2\nu G}{1-2\nu}\delta_{ij}\delta_{kl} + G(\delta_{ik}\delta_{jl} + \delta_{il}\delta_{jk}).$$

For the plastic part, we assume that

$$(2.4) \quad V^{(p)} = \lambda\Psi$$

where the symmetric tensor Ψ indicates the direction of plastic deformation in stress space (the flow rule). To describe the hardening process, we introduce a new unknown—the total plastic shear strain γ defined by

$$\gamma_t = |\text{dev } V^{(p)}|.$$

The multiplier λ in (2.4) can be obtained by differentiating the yield surface $\phi(T^{(s)}, \gamma) = 0$, which yields:

$$(2.5) \quad \Phi_{ij}\partial_t T_{ij}^{(s)} + \frac{\partial\phi}{\partial\gamma}\gamma_t = 0$$

where the symmetric tensor $\Phi = \partial\phi/\partial T^{(s)}$ is the normal direction to the yield surface. For convenience, we assume that Ψ and Φ are dimensionless and also normalized in the sense that:

$$|\text{dev } \Psi| = |\text{dev } \Phi| = 1.$$

It follows from (2.4), (2.5) that

$$(2.6) \quad \lambda = |\text{dev } V^{(p)}| = \partial_t \gamma = \frac{1}{h}\Phi_{ij}\partial_t T_{ij}^{(s)}$$

where

$$h = - \left(\frac{\partial \phi}{\partial \gamma} \right)^{-1}$$

is called the hardening modulus. Combining (2.2) with (2.3)–(2.6), we obtain

$$(2.7) \quad V = \left(C_{ijkl} + \frac{1}{h} \Psi_{ij} \Phi_{kl} \right) \partial_t T_{ij}^{(s)}.$$

Inverting (2.7) yields:

$$(2.8) \quad \partial_t T_{ij}^{(s)} = \left(E_{ijkl} - \frac{1}{H} (E_{ijmn} \Psi_{mn}) (\Phi_{rs} E_{rskl}) \right) V_{kl},$$

where

$$H = h + \Phi_{ij} E_{ijkl} \Psi_{kl}.$$

Substituting (2.8) in (2.5), we obtain

$$\partial_t \gamma = \left(\frac{1}{h} \Phi_{ij} \partial_t T_{ij}^{(s)} \right)_+ = \frac{1}{H} (\Phi_{ij} E_{ijkl} V_{kl})_+$$

where

$$(a)_+ = \begin{cases} a & \text{if } a > 0, \\ 0 & \text{if } a \leq 0. \end{cases}$$

In Cosserat theory, a new couple stress S is introduced which is related to the antisymmetric part $T^{(a)}$ of T through the conservation of angular momentum

$$\partial_k S_{kl} + e_{lmn} T_{mn}^{(a)} = 0,$$

where e_{lmn} is the alternating tensor with $e_{123} = 1$. As an extension of linear elasticity, the deviator of S satisfies the following constitutive relation:

$$\partial_t (\text{dev } S_{kl}) = 2\eta e_{lmn} \partial_k \omega_{mn} + 2\eta' e_{kmn} \partial_l \omega_{mn}$$

with $\eta > 0$ and $|\eta'| < \eta$, where

$$\omega_{kl} = \frac{1}{2} (\partial_k v_l - \partial_l v_k)$$

is the spin rate tensor. It follows that

$$(2.9) \quad \partial_t T_{ij}^{(a)} = -2\eta \partial_{kk} \omega_{ij} - \frac{1}{2\eta} \partial_t (\partial_l S_{kk}) e_{ijl}.$$

Similarly, we assume the following constitutive relation for p .

$$(2.10) \quad \partial_t p = -\zeta \partial_{kk} \partial_l v_l.$$

which relates the rate of change of the dispersive pressure to the rate of dilational change of the material. Together with (2.8)–(2.10), the constitutive relations can be rewritten as

$$\begin{aligned} \partial_t T_{ij} &= \left[E_{ijkl} - \frac{\chi}{H} (E_{ijmn} \Psi_{mn}) (\Phi_{rs} E_{rskl}) \right] V_{kl} \\ &\quad - \zeta \partial_{kk} \partial_l v_l \delta_{ij} - \eta \partial_{kk} (\partial_i v_j - \partial_j v_i), \\ \partial_t \gamma &= \frac{\chi}{H} (\Phi_{ij} E_{ijkl} V_{kl})_+ \end{aligned}$$

where the symbol χ is a characteristic function which is zero for $\phi(T^{(s)}, \gamma) < 0$ and one for $\phi = 0$.

Remark 2.1. We build the microstructure into the models through the elastic part (i.e. particles are connected by elastic springs) and as a result the effect is dispersive [4]. In general, microstructure should also be built into the plastic part which would result in dissipative effects.

It is true that, for some critical values of the hardening modulus, the system (2.1) without microstructure [12], [13], [2], [3], [6] will lose hyperbolicity with respect to plane waves in certain directions. There are two types of ill-posedness: shear-band and flutter ill-posedness. In this paper, we restrict our analysis to shear-band ill-posedness in simple models. Analysis for general cases (at least having two velocity components, or dealing with flutter ill-posedness) will be given in future work.

3. A weakly nonlinear approximation of two model problems. In this section we consider two special cases of the above elasto-plastic model with microstructure. The first corresponds to the longitudinal motion of an elasto-plastic bar while the second corresponds to anti-plane shear deformation. We perform a perturbation expansion about the critical state associated with the onset of instability and analyze the nonlinear equations obtained by retaining second order perturbations.

3.1. Longitudinal motion of an elasto-plastic bar. In this case we have

$$(\partial_x v)^{(e)} = \frac{1}{G} \partial_t T, \quad (\partial_x v)^{(p)} = \lambda = \partial_t \gamma.$$

So the constitutive law is

$$\partial_x v = \frac{1}{G} \partial_t T + \partial_t \gamma.$$

It follows from the yield condition $T = g(\gamma)$ (we only consider the tensile case $T > 0$) that

$$\partial_t \gamma = \left(\frac{1}{g'(\gamma)} \partial_t T \right)_+ = \frac{G}{G + g'} (\partial_x v)_+$$

where the function $g(\gamma)$ is shown in Fig. 3.1. We observe that, for this problem, points on the yield surface will undergo further plastic deformation when $\partial_x v > 0$, while points on the yield surface will undergo elastic deformation when $\partial_x v < 0$.

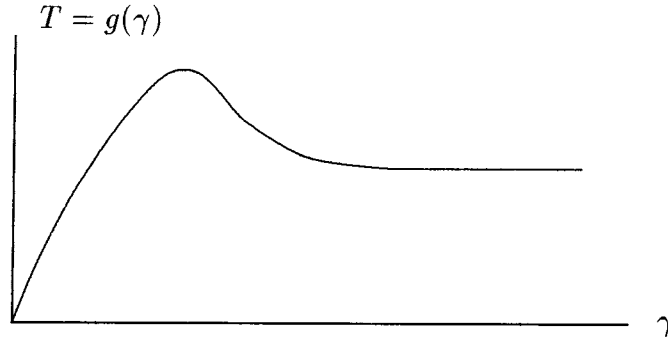


FIG. 3.1. The yield stress as a function of the total shear strain γ .

For easy reference, we rewrite the complete system as follows:

$$(3.1) \quad \begin{aligned} \rho \partial_t v &= \partial_x T, \\ \partial_t T &= G \partial_x v - G \partial_t \gamma - \zeta \partial_{xxx} v, \\ \partial_t \gamma &= \begin{cases} \frac{G}{G+g'} (\partial_x v)_+ & \text{if } T = g(\gamma), \\ 0 & \text{if } T < g(\gamma). \end{cases} \end{aligned}$$

The third-order term comes from the dispersive pressure alone. Without this term, we obtain the following nonlinear wave equation

$$(3.2) \quad \rho \partial_{tt} v = \left(\frac{Gg'}{G+g'} \partial_x v \right)_x,$$

when the material is undergoing plastic deformation. It is clear that the equation (3.2) (or equivalently the system (3.1) without the third-order term) will change type when g' becomes negative. Thus there is a critical state (γ_c, T_c) such that

$$g'(\gamma_c) = 0, \quad T_c = g(\gamma_c).$$

We now assume small perturbations about the critical state of the form:

$$T = T_c + \bar{T}, \quad \gamma = \gamma_c + \bar{\gamma}, \quad v = \bar{v},$$

which we substitute into (3.1) to obtain

$$\begin{aligned} \rho \bar{v}_t &= \bar{T}_x \\ \bar{T}_t &= G \bar{v}_x - G \bar{\gamma}_t - \zeta \bar{v}_{xxx} \\ \bar{\gamma}_t &= \left(1 - \frac{1}{G} g'' \bar{\gamma} \right) \bar{v}_x \\ &= \left(1 - \frac{1}{G} g'' \int_{t_0}^t \bar{v}_x d\tau \right) \bar{v}_x, \end{aligned}$$

where the fact that $g'(\gamma_c) = 0$ has been used. We note that $g''(\gamma_c) < 0$ since $g(\gamma_c)$ is a maximum. In the plastic region ($\bar{v}_x > 0$), we have, by eliminating $\bar{\gamma}$

$$(3.3) \quad \rho \bar{v}_t = \bar{T}_x, \quad \bar{T}_t = g'' \left(\int_{t_0}^t \bar{v}_x d\tau \right) \bar{v}_x - \zeta \bar{v}_{xxx}.$$

Note that the integral in (3.3) represents history-dependence of the plastic deformation.

Similarly, in the elastic region ($\bar{\gamma} \equiv 0$) we obtain

$$\rho \bar{v}_t = \bar{T}_x, \quad \bar{T}_t = G \bar{v}_x - \zeta \bar{v}_{xxx}.$$

For the purpose of analysis, it is convenient to remove this explicit history-dependence by expressing the problem in terms of displacements instead of velocities. Let

$$u = \int_{t_0}^t \bar{v} d\tau.$$

Dropping the bars, the system in the plastic region then becomes:

$$(3.4) \quad \begin{aligned} \text{(a)} \quad \rho u_{tt} &= T_x \\ \text{(b)} \quad T_t &= g'' u_x u_{xt} - \zeta u_{xxxx}, \end{aligned}$$

while in the elastic region we have:

$$(3.5) \quad \begin{aligned} (a) \quad & \rho u_{tt} = T_x \\ (b) \quad & T_t = G u_{xt} - \zeta u_{xxxxt}. \end{aligned}$$

Eliminating T in (3.4), we obtain:

$$(3.6) \quad \rho u_{tt} = \frac{g''}{2} (u_x^2)_x - \zeta u_{xxxx} + f_{1x}(x).$$

It is easy to check that u_x satisfies the Boussinesq equation [1], [9] (provided $f_{1x} = 0$), one of the completely integrable nonlinear PDE which has solutions exhibiting a soliton structure.

3.2. Anti-plane shearing. In this subsection (cf. [14]), we consider the special case of the general elasto-plastic equations in which the unknowns are assumed to be of the special form $v = v_3(x_1, x_2)$, $T = (T_1, T_2) = (T_{31}, T_{32})$ and γ .

The strain-stress relations are as follows:

$$(3.7) \quad \begin{aligned} (a) \quad & (\text{grad } v)^{(e)} = \frac{1}{G} \partial_t T^{(s)} \\ (b) \quad & (\text{grad } v)^{(p)} = \lambda \frac{RT^{(s)}}{|T^{(s)}|}, \end{aligned}$$

where the rotation matrix

$$R = \begin{pmatrix} \cos \alpha & \sin \alpha \\ -\sin \alpha & \cos \alpha \end{pmatrix}$$

has been included into the constitutive law to model a nonassociative flow rule in the case $\alpha \neq 0$. Differentiating the yield function $\phi(T^{(s)}, \gamma) = |T^{(s)}| - g(\gamma) = 0$, we have

$$(3.8) \quad \partial_t \gamma = \frac{1}{g'(\gamma)} \left\langle \frac{T^{(s)}}{|T^{(s)}|}, \partial_t T^{(s)} \right\rangle.$$

It follows from (3.7.b) that

$$\lambda = |\text{grad } v^{(p)}| = \partial_t \gamma = \frac{1}{g'(\gamma)} \left\langle \frac{T^{(s)}}{|T^{(s)}|}, \partial_t T^{(s)} \right\rangle.$$

Hence

$$\text{grad } v = \frac{1}{G} \left[I + \frac{G}{g'(\gamma)} \frac{(RT^{(s)})(T^{(s)})^T}{|T^{(s)}|^2} \right] \partial_t T^{(s)}.$$

Inverting we obtain

$$\partial_t T^{(s)} = G \left[I - \frac{1}{H} \frac{(RT^{(s)})(T^{(s)})^T}{|T^{(s)}|^2} \right] \text{grad } v,$$

where

$$H = \frac{g'}{G} + \frac{\langle RT^{(s)}, T^{(s)} \rangle}{|T^{(s)}|^2} = \frac{g'}{G} + \cos \alpha.$$

Substituting this relation into (3.8), we have

$$\partial_t \gamma = \frac{1}{H} \left\langle \frac{T^{(s)}}{|T^{(s)}|}, \text{grad } v \right\rangle_+.$$

For easy reference, we summarize the governing equations in this special case:

$$(3.9) \quad \begin{aligned} \rho \partial_t v &= \partial_{x_1} T_1 + \partial_{x_2} T_2, \\ \partial_t T &= G \left[I - \frac{1}{H} \frac{\langle RT^{(s)}, T^{(s)} \rangle}{|T^{(s)}|^2} \right] \text{grad } v - \eta \text{grad}(\partial_{kk} v), \\ \partial_t \gamma &= \frac{1}{H} \left\langle \frac{T^{(s)}}{|T^{(s)}|}, \text{grad } v \right\rangle_+. \end{aligned}$$

Note that, in this case, the third-order term comes from Cosserat theory alone. It was found [14] that the system loses its hyperbolicity if and only if

$$\begin{aligned} & \min_{|\xi|=1} \xi^T \left[I - \frac{1}{H} \frac{(RT^{(s)})(T^{(s)})^T}{|T^{(s)}|^2} \right] \xi \\ &= \min_{|\xi|=1} \frac{1}{H} \left(H - \langle \xi, RT^{(s)} \rangle \langle \xi, T^{(s)} \rangle \right) = \frac{1}{H} \left(\frac{g'}{G} - \sin^2 \frac{\alpha}{2} \right) \end{aligned}$$

is negative where $\xi = (\xi_1, \xi_2)$ is the wave number. Moreover, under uniform deformation

$$v(x_1, x_2, t) = x_1, \quad T^{(s)}(x_1, x_2, t) = T^{(s)}(t),$$

and the appropriate choice of initial conditions, the solution first loses stability to plane wave perturbations in the x_1 -direction. In this case, the equations lose hyperbolicity when

$$T^{(s)} = |T_c^{(s)}| \left(\cos \frac{\alpha}{2}, \sin \frac{\alpha}{2} \right), \quad \gamma = \gamma_c$$

at which

$$g'(\gamma_c) = G \sin^2 \frac{\alpha}{2}, \quad |T_c^{(s)}| = g(\gamma_c).$$

It is possible to assume that the unknowns are functions of x_1 only (in what follows we simply write x for x_1). The system (3.9) in the plastic region is as follows:

$$(3.10) \quad \begin{aligned} (a) \quad & \rho \partial_t v = \partial_x T_1 \\ (b) \quad & \partial_t T_1 = \frac{G}{H} \left[\frac{g'}{G} - \frac{T_2^{(s)}}{|T^{(s)}|^2} \left(T_1^{(s)} \sin \alpha - T_2^{(s)} \cos \alpha \right) \right] \partial_x v - \eta \partial_{xxx} v \\ (c) \quad & \partial_t T_2 = \frac{G}{H} \frac{T_1^{(s)}}{|T^{(s)}|^2} \left(T_1^{(s)} \sin \alpha - T_2^{(s)} \cos \alpha \right) \partial_x v \\ (d) \quad & \partial_t \gamma = \frac{1}{H} \left\langle \frac{T_1^{(s)}}{|T^{(s)}|}, \partial_x v \right\rangle_+; \end{aligned}$$

while in the elastic region,

$$\begin{aligned} \rho \partial_t v &= \partial_x T_1, \\ \partial_t T_1 &= G \partial_x v - \eta \partial_{xxx} v, \\ \partial_t T_2 &= 0, \quad \partial_t \gamma = 0. \end{aligned}$$

As before we assume the perturbation expansion:

$$T = T_c^{(s)} + \bar{T}, \quad v = \bar{v}, \quad \gamma = \gamma_c + \bar{\gamma}.$$

By Taylor expansion,

$$\frac{g'}{G} - \frac{T_2^{(s)}}{|T^{(s)}|^2} \left(T_1^{(s)} \sin \alpha - T_2^{(s)} \cos \alpha \right) = \frac{g''}{G} \bar{\gamma} + 0 \cdot \bar{T}_1^{(s)} + 0 \cdot \bar{T}_2^{(s)}.$$

It follows from (3.10.d) that

$$\bar{\gamma} = \frac{1}{\cos \frac{\alpha}{2}} \int_{t_0}^t \partial_x \bar{v} d\tau.$$

Thus the equation (3.10.b) becomes

$$(3.11) \quad \partial_t \bar{T}_1 = \frac{g''}{\cos \frac{\alpha}{2}} \int_{t_0}^t \partial_x \bar{v} d\tau \cdot \partial_x \bar{v} - \eta \partial_{xxx} \bar{v}.$$

Letting

$$u = \int_{t_0}^t \bar{v} d\tau,$$

and integrating (3.11) with respect to t once, we obtain

$$\bar{T}_1 = \frac{g''}{2 \cos \frac{\alpha}{2}} (u_x)^2 - \eta \partial_{xxx} u.$$

Combining with (3.10.a), we have

$$\rho \partial_{tt} u = \frac{g''}{2 \cos \frac{\alpha}{2}} (u_x^2)_x - \eta \partial_{xxxx} u$$

which, up to the factor $\cos \frac{\alpha}{2}$, is the Boussinesq equation we obtained in the previous subsection.

4. Special solutions and jump profile. In this section we derive some explicit solutions of the equation (3.6). We assume that $f_{1x} = 0$. It is clear that $u = \text{const}$ and $u_x = \text{const}$ are solutions of

$$(4.1) \quad \rho u_{tt} = \frac{g''}{2} (u_x^2)_x - \zeta u_{xxxx}.$$

Now we look for a traveling wave solution of the form

$$u = U(\xi), \quad \xi = x \pm ct.$$

It follows from (3.6) that

$$c^2 \rho U'' = \frac{g''}{2} (U'^2)' - \zeta U''''.$$

Integrating once we obtain

$$c^2 \rho U' = \frac{g''}{2} U'^2 - \zeta U''' + A.$$

Multiplying by U'' , integrating and letting $z = U'$ we obtain

$$\frac{c^2 \rho z^2}{2} = \frac{g''}{6} z^3 - \frac{\zeta}{2} z'^2 + Az + B.$$

Solving for z' we obtain

$$z'^2 = -\frac{g''}{3\zeta} \left[-z^3 + \frac{3c^2\rho}{g''}z^2 - \frac{6A}{g''}z - \frac{6B}{g''} \right].$$

If the constants A and B are chosen so that the cubic in z on the right-hand side of the above ODE has three real roots, then z will be periodic and can be expressed in terms of Jacobian elliptic functions. These periodic solutions are not suitable for our objective of obtaining jump profiles. However, if we choose A and B , such that

$$-z^3 + \frac{3c^2\rho}{g''}z^2 - \frac{6A}{g''}z - \frac{6B}{g''} = (z - z_1)^2(z_2 - z)$$

where z_1 and z_2 satisfy

$$(4.2) \quad z_2 > 0 > z_1 \quad \text{and} \quad 2z_1 + z_2 = \frac{3c^2\rho}{g''}.$$

In this case

$$\frac{dz}{(z - z_1)\sqrt{z_2 - z}} = \pm \sqrt{\frac{-g''}{3\zeta}} d\xi.$$

Making use of the indefinite integral

$$\int \frac{dz}{(z - z_1)\sqrt{z_2 - z}} = -\frac{2}{\sqrt{z_2 - z_1}} \operatorname{sech}^{-1} \left(\sqrt{\frac{z - z_1}{z_2 - z_1}} \right),$$

it follows that

$$z - z_1 = (z_2 - z_1) \operatorname{sech}^2 \left(\frac{1}{2\sqrt{3}} \sqrt{\frac{-g''(z_2 - z_1)}{\zeta}} (\xi - \xi_0) \right).$$

Since we are considering shear-band ill-posedness, which corresponds to a stationary “jump” in the displacement, we let $c = 0$. It follows from (4.2) that $z_2 = -2z_1$. Therefore,

$$(4.3) \quad u_x = z_1 \left\{ 1 - 3 \operatorname{sech}^2 \left[\frac{1}{2} \sqrt{\frac{g'' z_1}{\zeta}} (x - x_0) \right] \right\},$$

which is shown in Fig. 4.1. The plastic part of the solution is denoted by the solid bell-shaped curve between x_2 and x_1 , while the dashed curves denote the extension of this solution beyond its region of validity into the elastic region. In order to determine where to patch the elastic and plastic solutions, we search for those points, x_1 and x_2 , at which u_x changes sign.

It follows from (4.3) that $u_x(x_1) = u_x(x_2) = 0$ where

$$x_{1,2} = x_0 \pm 2 \sqrt{\frac{\zeta}{g'' z_1}} \cosh^{-1}(\sqrt{3}).$$

The second derivative of u at $x_{1,2}$ is equal to

$$u_{xx}|_{x=x_{1,2}} = z_1 \sqrt{\frac{2g'' z_1}{3\zeta}} \operatorname{sgn}(x_{1,2} - x_0).$$

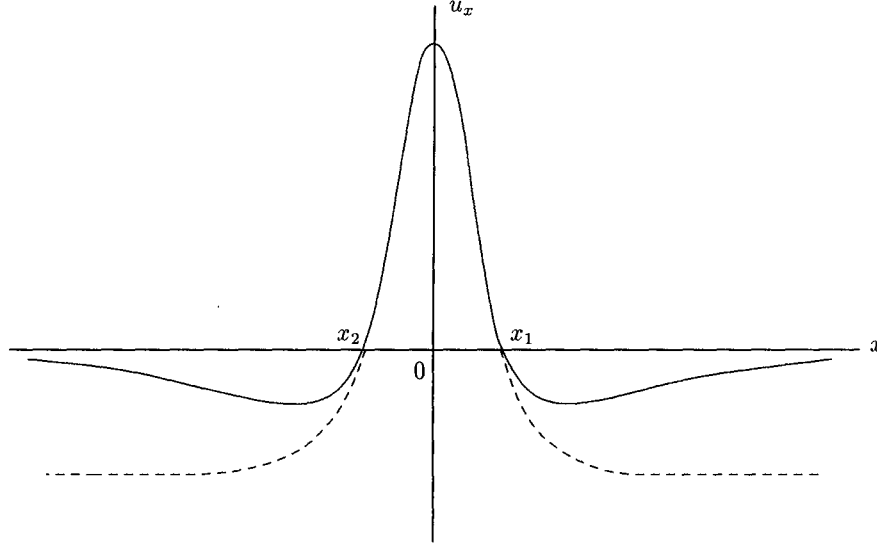


FIG. 4.1. The gradient of the displacement: a stationary solution to the simplified equations. The dashed curves represent the extension of the solution in the plastic region.

For the elastic region we look for the solution to (3.5). Eliminating T we obtain

$$\rho u_{tt} = G u_{xx} - \zeta u_{xxxx} + f_2(x)$$

where f_2 is an arbitrary function of x . Time-independent solutions to this equation satisfy

$$u_{xxx} = \frac{G}{\zeta} u_x - f_2(x).$$

The solution to this equation is given by

$$u_x = C_1 \exp\left(\sqrt{\frac{G}{\zeta}}x\right) + C_2 \exp\left(-\sqrt{\frac{G}{\zeta}}x\right) - \sqrt{\frac{\zeta}{G}} \int_x^{+\infty} \sinh\left(\sqrt{\frac{G}{\zeta}}(x-y)\right) f_2(y) dy.$$

If we require $u_x(+\infty) = 0$, then for $x > x_1$, we have

$$u_x = C_2 \exp\left(-\sqrt{\frac{G}{\zeta}}(x-x_1)\right) - \sqrt{\frac{\zeta}{G}} \int_x^{+\infty} \sinh\left(\sqrt{\frac{G}{\zeta}}(x-y)\right) f_2(y) dy.$$

The condition $u_x(x_1) = 0$ yields

$$C_2 = \sqrt{\frac{\zeta}{G}} \int_{x_1}^{+\infty} \sinh\left(\sqrt{\frac{G}{\zeta}}(x_1-y)\right) f_2(y) dy.$$

The second derivative of u at x_1 is given by

$$u_{xx}|_{x=x_1^+} = - \int_{x_1}^{+\infty} \exp\left(\sqrt{\frac{G}{\zeta}}(x_1-y)\right) f_2(y) dy.$$

By an appropriate choice of $f_2(y)$, we can make $u_{xx}|_{x=x_1^-} = u_{xx}|_{x=x_1^+}$, i.e.,

$$z_1 \sqrt{\frac{2g''z_1}{3\zeta}} \operatorname{sgn}(x_1 - x_0) = - \int_{x_1}^{\infty} \exp\left(\sqrt{\frac{G}{\zeta}}(x_1 - y)\right) f_2(y) dy.$$

Similarly, we can find an expression for u in the region $x < x_2$. The function u_x is shown in Fig. 4.1. The dashed curves represent the extension of the Boussinesq solution u_x beyond the plastic region. The function u , which is obtained by integrating u_x , is shown in Fig. 4.2. The dashed curves represent the extension of u beyond the plastic region.

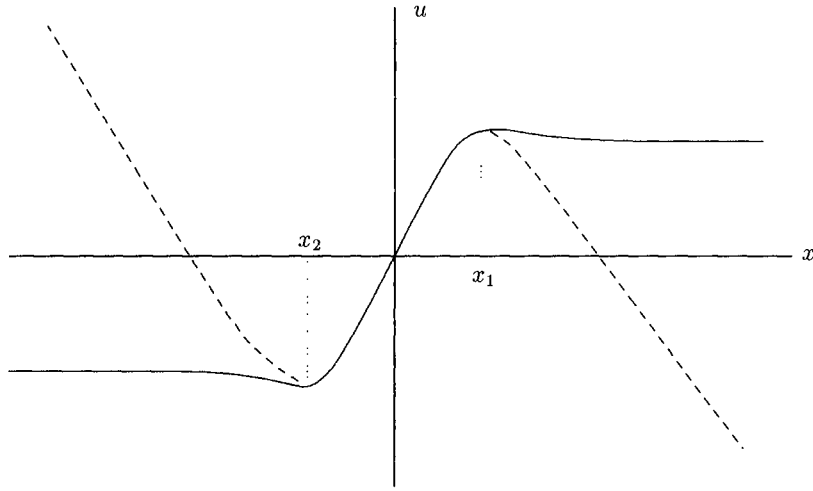


FIG. 4.2. The displacement obtained from integration of u_x . The dashed curves represent the extension of the integration in the plastic region.

Without microstructure, solutions will have a jump at $x = x_0$. In order to get a well-posed model, certain jump conditions need to be imposed. As we mentioned in the introduction, the constitutive relation cannot be written in conservation form. Therefore the quantity to be conserved across the jump cannot be determined directly from the equations without microstructure. In order to obtain the correct jump structure, we consider the small microstructure limit of the microstructure equations. This approach is analogous to the small viscosity limit [15] used to derive the jump structure for conservation laws. In order that the jump be finite, we require that the height of the jump should be independent of ζ . In our problem, the height of the jump is equal to the integral of (4.3) from x_2 to x_1 .

$$\begin{aligned} L &= \int_{x_2}^{x_1} u_x(x) dx = -z_1 \int_{x_2}^{x_1} \left\{ 1 - 3 \operatorname{sech}^2 \left(\frac{1}{2} \sqrt{\frac{g''z_1}{\zeta}} (x - x_0) \right) \right\} dx \\ &= -2z_1 \int_0^{\bar{x}_1} \left\{ 1 - 3 \operatorname{sech}^2 \left(\frac{1}{2} \sqrt{\frac{g''z_1}{\zeta}} x \right) \right\} dx \end{aligned}$$

where $\bar{x}_1 = 2\sqrt{\frac{\zeta}{g''z_1}} \cosh^{-1}(\sqrt{3})$. After changing variables in the above integral we obtain

$$L = 4\sqrt{\frac{\zeta z_1}{g''}} \int_0^{\cosh^{-1}(\sqrt{3})} (3 \operatorname{sech}^2(y) - 1) dy.$$

If $z_1 \sim \frac{C}{\zeta}$, then L is independent of ζ . As a result

$$x_2 - x_1 = 4\sqrt{\frac{\zeta}{g''z_1}} \cosh^{-1}(\sqrt{3}) \sim \hat{C}\zeta.$$

Alternatively, the same result can be obtained by rescaling variables in the equation:

$$\frac{g''}{2}(u_x^2)_x = \zeta u_{xxxx}.$$

If we let $X = \zeta^\alpha x$, then the equation becomes

$$\frac{g''}{2}\zeta^{3\alpha}(u_X^2)_X = \zeta^{1+4\alpha}u_{XXXX}.$$

The relation $3\alpha = 1 + 4\alpha$ implies that $\alpha = -1$ from which it follows that $x = \zeta X$.

This special solution assumes that the stress T is in an equilibrium state. Therefore the above limiting process which we used to obtain the jump structure will only apply to loading paths in which the stress T reaches an equilibrium state at values of the total plastic shear strain γ which are close enough to the critical state for the weakly nonlinear approximation to be valid. In general T will ultimately move to the constant stress state characterized by the flat part of the yield curve (cf. Fig. 3.1). However, the values of γ at this stage will be beyond the region of validity of the weakly nonlinear approximation so the jump conditions will no longer apply.

Remark 4.1. The assumption that $f_{1x} = 0$ in (3.6) allows us to construct solutions easily. The vanishing of f_{1x} in (3.6) only affects the zeroth order nominal solution but does not affect the stability analysis.

5. Instability of special solutions.

5.1. Multiple scales analysis of the constant displacement solution.

In this subsection, we carry out the multiple scales analysis described in [10] for the equation

$$(5.1) \quad u_{tt} + au_x u_{xx} + \zeta u_{xxxx} = 0.$$

Essentially, this method generates a hierarchy of linear differential equations from which secular terms are removed.

Suppose that

$$(5.2) \quad u(x, t) = \sum_{n=1}^{\infty} \epsilon^n u^{(n)}(X_0, X_1, T_0, T_1, T_2) + u^{(0)}$$

where $u^{(0)} \equiv \text{const}$ and

$$(5.3) \quad X_k = \epsilon^k x, \quad k = 0, 1 \quad \text{and} \quad T_k = \epsilon^k t, \quad k = 0, 1, 2.$$

The fast scales in time and space correspond to $k = 0$ while the longer space and slower time scales correspond to the higher values of k . Using the chain rule for

differentiation, we obtain

$$(5.4) \quad \frac{\partial}{\partial x} = \sum_{n=0}^1 \epsilon^n \frac{\partial}{\partial X_n}, \quad \frac{\partial}{\partial t} = \sum_{n=0}^2 \epsilon^n \frac{\partial}{\partial T_n}.$$

Substituting (5.2)–(5.4) into (5.1) and collecting terms with equal powers of ϵ , we generate a hierarchy of equations of which the first three members are

$$(5.5) \quad Lu^{(1)} = 0,$$

$$(5.6) \quad Lu^{(2)} = -2\partial_{T_0 T_1} u^{(1)} - a\partial_{X_0} u^{(1)} \partial_{X_0 X_0} u^{(1)} - 4\zeta \partial_{X_0 X_0 X_0 X_1} u^{(1)},$$

$$(5.7) \quad Lu^{(3)} = -(\partial_{T_0 T_2} + \partial_{T_1 T_1})u^{(1)} - 2\partial_{T_0 T_1} u^{(2)} - 2\zeta(3\partial_{X_1 X_1 X_0 X_0} u^{(1)} + 2\partial_{X_0 X_0 X_0 X_1} u^{(2)}) - a \left[\partial_{X_0} u^{(1)} \left(2\partial_{X_0 X_1} u^{(1)} + \partial_{X_0 X_0} u^{(2)} \right) + \partial_{X_0 X_0} u^{(1)} \left(\partial_{X_1} U^{(1)} + \partial_{X_0} u^{(2)} \right) \right]$$

where L is the linear operator (the beam equation)

$$(5.8) \quad L := \frac{\partial^2}{\partial T_0^2} + \zeta \frac{\partial^4}{\partial X_0^4}.$$

Now consider a solution of (5.5) of the form

$$(5.9) \quad u^{(1)} = \sum_{j=1}^2 A_j(X_1, T_1, T_2) e^{i\theta_j} + A_j^*(X_1, T_1, T_2) e^{-i\theta_j}$$

where A^* is the complex conjugate of A and

$$\theta_j = kX_0 - \omega_j T_0, \quad j = 1, 2.$$

For (5.9) to be a solution of (5.5), the wave frequency ω and the wave number k have to satisfy the following dispersion relation:

$$\omega_j = (-1)^{j-1} \sqrt{\zeta} k^2, \quad j = 1, 2.$$

When the problem is considered in a bounded domain, the choice of the wave numbers will be discrete. Substituting (5.9) in (5.6), we obtain

$$(5.10) \quad Lu^{(2)} = \sum_{j=1}^2 \left\{ i e^{i\theta_j} \left(2\partial_{T_1} A_j \omega_j + 4\zeta k^3 \partial_{X_1} A_j \right) - i e^{-i\theta_j} \left(2\omega_j \partial_{T_1} A_j^* + 4\zeta k^3 \partial_{X_1} A_j^* \right) + ai \left(A_j^2 e^{2i\theta_j} - A_j^{*2} e^{-2i\theta_j} \right) \right\}.$$

To remove secular terms, we impose the condition

$$(5.11) \quad \partial_{T_1} A_j \omega_j + 2\zeta k^3 \partial_{X_1} A_j = 0, \quad j = 1, 2.$$

We then find that (5.10) has a solution of the form

$$(5.12) \quad u^{(2)} = \sum_{j=1}^2 \frac{ia}{12\zeta k^4} \left(A_j^2 e^{2i\theta_j} - A_j^{*2} e^{-2i\theta_j} \right).$$

Substituting (5.9) and (5.12) in (5.7), we find that secular terms can be removed by imposing the condition

$$(5.13) \quad -i\omega_j \partial_{T_2} A_j + \partial_{T_1 T_1} A_j - 6\zeta k^2 \partial_{X_1 X_1} A_j - \frac{a^2}{6\zeta k} A_j |A_j|^2 = 0.$$

It follows from (5.11) that

$$\partial_{T_1 T_1} A_j = 4\zeta k^2 \partial_{X_1 X_1} A_j.$$

Thus, (5.13) becomes

$$\partial_{T_2} A_j - i(-1)^{j-1} \left[2\sqrt{\zeta} \partial_{X_1 X_1} A_j + \frac{a^2}{6\zeta\sqrt{\zeta}k^3} A_j |A_j|^2 \right] = 0, \quad j = 1, 2$$

which is the nonlinear Schrödinger equation in the variables T_2 , X_1 . It was shown (see, for instance, [16]) that the envelope A_j is unstable, since coefficients of the second two terms have the same sign.

5.2. Instability of the constant strain solution. In this case, it is not necessary to carry out a delicate multiple scales analysis in order to detect instabilities since instabilities occur even in the fast scales in time and space.

We assume that $u_x(0) \equiv c > 0$, since the equation only holds in the plastic region. The linearized equation is

$$(5.14) \quad u_{tt} + au_x^{(0)} u_{xx} + \zeta u_{xxxx} = 0.$$

Without the microstructure term ($\zeta = 0$), the initial value problem is ill-posed. With the microstructure term, the initial value problem becomes well-posed but some of the Fourier modes may still be unstable. In fact, substituting $u = \hat{u}e^{ix\xi + \lambda t}$ in (5.14), we obtain

$$\lambda^2 + ac(i\xi)^2 + \zeta(i\xi)^4 = 0.$$

It follows that

$$\text{Re}(\lambda_{1,2}) = |\xi| \sqrt{ac - \zeta\xi^2} H(ac - \zeta\xi^2)$$

where H is the Heaviside function. The solution to (5.14) will be unstable with respect to low Fourier modes

$$|\xi| \leq \sqrt{\frac{ac}{\zeta}}.$$

5.3. Instability of soliton solutions. The linearized equation around the soliton solution is

$$(5.15) \quad u_{tt} + au_x^{(0)} u_{xx} + au_{xx}^{(0)} u_x + \zeta u_{xxxx}$$

where $u^{(0)} = u^{(0)}(x)$ is the solution obtained in §4. Again, we only look at the region where $u_x^{(0)} > 0$.

Substituting $u = \hat{u}e^{ix\xi + \lambda t}$ in (5.15), we obtain

$$\lambda^2 = \xi^2 (au_x^{(0)} - \zeta\xi^2) - iau_{xx}^{(0)}\xi,$$

from which it follows that

$$|\text{Re}(\lambda_{1,2})| = \frac{1}{\sqrt{2}} \left\{ \sqrt{\xi^4 (au_x^{(0)} - \zeta\xi^2)^2 + (au_{xx}^{(0)}\xi)^2} + (au_x^{(0)} - \zeta\xi^2)\xi^2 \right\}^{1/2},$$

which satisfies

$$\begin{aligned} |\operatorname{Re}(\lambda_{1,2})| &\sim \frac{1}{\sqrt{2}} \sqrt{a|u_{xx}^{(0)}| |\xi|} \quad \text{as } \xi \rightarrow 0 \\ |\operatorname{Re}(\lambda_{1,2})| &\sim \frac{a|u_{xx}^{(0)}|}{2\sqrt{\zeta}|\xi|} \quad \text{as } \xi \rightarrow \infty. \end{aligned}$$

Note that, this argument can be justified by the previous multiple scales analysis when $u_x^{(0)}$ and $u_{xx}^{(0)}$ do not change too rapidly in x (at least in the interior of the plastic region).

From the stability analyses of the above three special solutions, we conclude that when the stress is just beyond the critical state the solution is unstable and the amplitudes of the lower wave-numbers grow. This phenomenon is a net result of competition between the focusing effect of the nonlinearity and the dispersive effect of the microstructure terms. The nonlinearity provides a self-focusing effect which, if it were not inhibited by the microstructure terms, would cause uncontrolled growth of arbitrarily fine scales. The microstructure terms inhibit the uncontrolled growth of the highest wave-numbers which means that only the lower wave-numbers (which fall within the limits of the continuum assumption) can grow. The growth of these physically relevant wave-numbers ultimately leads to the formation of shear bands. These conclusions only apply in the region of validity $|\gamma - \gamma_0| \ll 1$ of the small perturbation analysis that was used to derive (5.1). If the plastic strain γ is much larger than γ_0 (see for example the flat part of the $\gamma - T$ curve in Fig. 3.1), then stress state could become constant and in this case the velocity will reach a stable jump profile. However, in this case (5.1) is no longer valid—in fact the velocity in this regime satisfies the beam equation and the nonlinear term disappears.

6. Numerical experiments. Here we only present some numerical experiments on the perturbed equation (5.1) and its elastic counterpart. Further numerical results for the complete system (3.1) will be given in another paper [5] in which the process from uniform deformation to localization is demonstrated.

In the plastic region ($u_{j+1}^n > u_{j-1}^n$), we employ the difference approximation:

$$\begin{aligned} (6.1) \quad u_j^{n+1} &= 2u_j^n - u_j^{n-1} - \left(\frac{\Delta t}{\Delta x}\right)^2 \frac{a}{2\Delta x} (u_{j+1}^n - u_{j-1}^n)(u_{j+1}^n + u_{j-1}^n - 2u_j^n) \\ &\quad - \zeta \frac{\Delta t^2}{\Delta x^4} (u_{j+2}^n + u_{j-2}^n - 4u_{j+1}^n - 4u_{j-1}^n + 6u_j^n); \end{aligned}$$

while in the elastic region ($u_{j+1}^n \leq u_{j-1}^n$), we use

$$\begin{aligned} (6.2) \quad u_j^{n+1} &= 2u_j^n - u_j^{n-1} + \left(\frac{\Delta t}{\Delta x}\right)^2 (u_{j+1}^n + u_{j-1}^n - 2u_j^n) \\ &\quad - \zeta \frac{\Delta t^2}{\Delta x^4} (u_{j+2}^n + u_{j-2}^n - 4u_{j+1}^n - 4u_{j-1}^n + 6u_j^n). \end{aligned}$$

To guarantee stability in the elastic region, it is necessary to require that

$$(6.3) \quad \Delta t < \frac{(\Delta x)^2}{\sqrt{(\Delta x)^2 + 8\zeta}}.$$

In order to derive this condition, we substitute

$$u_j^n = \lambda^n e^{ijk\Delta x}$$

into (6.2) to obtain

$$\lambda^2 - 2 \left\{ 1 + (1 - \cos(k\Delta x)) \left(\frac{\Delta t}{\Delta x} \right)^2 + \frac{4\zeta(\Delta t)^2}{(\Delta x)^4} (1 - \cos(k\Delta x))^2 \right\} \lambda + 1 = 0.$$

The condition (6.3) follows from the requirement $|\lambda| \leq 1$.

In our computation, we assume that $a = 0.5$, $\zeta = 0.005$, and $\Delta x = 0.01$. We also use the boundary condition $\frac{\partial u}{\partial x}|_{x=0,1} = 0$ and the initial condition

$$u(x, 0) = \tan^{-1}(10(x - 0.5)) \left[1 - 0.3 \exp\left(-\frac{20}{20(x - 0.5)^2 + 1}\right) \right].$$

In Figs. 6.1 and 6.2, we see that, after $t = 0.05$, the amplitude of the jump grows significantly. Since the microstructure terms have been included in this model, amplitude growth is only restricted to the lower wave-numbers and as a result the displacement curve is quite smooth. In Figs. 6.3 and 6.4, we start with the same initial data but exclude the microstructure term. By time $t = 0.029$ we observe spontaneous jumps in the displacement profile which correspond the uncontrolled growth of the large wave-numbers. These jumps develop into numerical overflows almost immediately after this time-step. These results are consistent with the conclusions of our stability analysis in §5 and our previous conjecture.

7. Conclusions. The nonlinear equations of elasto-plastic flow are known to exhibit ill-posedness for certain values of the hardening parameter. The nonlinearity in the model, which in this context tracks the damage history of the material through the accumulation of plastic strain, provides a self-focusing mechanism. Without microstructure this term would make the initial value problem ill-posed which is characterized by the uncontrolled growth of the higher frequency modes. As a result infinitely fine-scale deformations are mobilized, which ultimately violate the continuum assumption of the model. The effects of such microscale deformations are built into the original continuum model by including the appropriate higher order dispersive terms. Previous studies of ill-posedness in elasto-plastic models and of the stability of elasto-plastic-micromodels have been restricted to linear analyses. Linear analysis shows that incorporating the microstructure terms into the model makes the problem well posed and leads to a stably growing profile for the displacement.

In this paper we used a weakly nonlinear analysis to explore the immediate post-critical behavior of elasto-plastic-micromodels. By considering small perturbations of the model equations about the critical state, we demonstrated that the gradient of displacement field satisfies the Boussinesq equation—one of the completely integrable PDE having soliton solutions. We used the Boussinesq equation, governing the evolution of small perturbations to the critical state, to explore two distinct features of the post-critical behavior of the solution. Firstly, we patched the special soliton solution in the plastic region to the solution in the elastic regions and were able to obtain the correct jump structure for certain loading paths. Secondly, we consider the stability properties of perturbations to certain special solutions. With help of multiple scale analysis we were able to show that a perturbation to a constant displacement solution is unstable on a slow time-scale. While perturbations to more complicated special solutions such as the constant strain solution and the soliton solution are unstable on

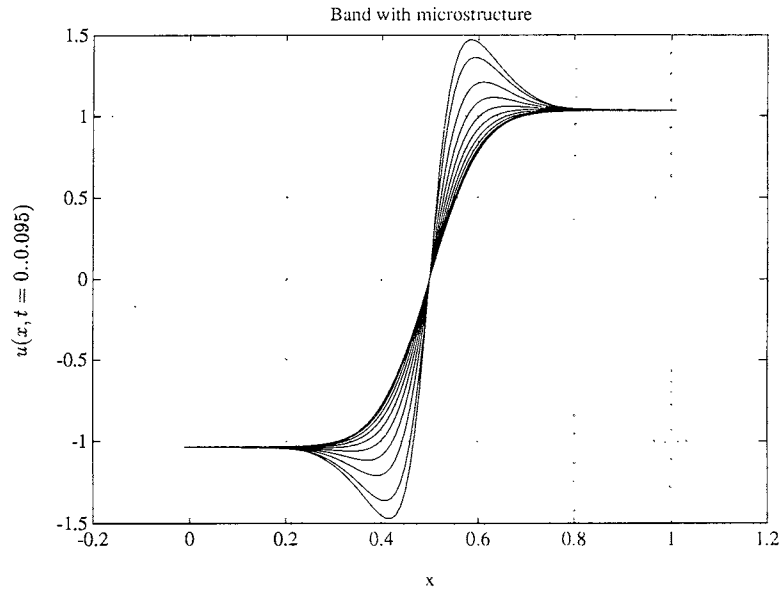


FIG. 6.1. The displacement curves (with microstructure) which are shown at different time-steps.

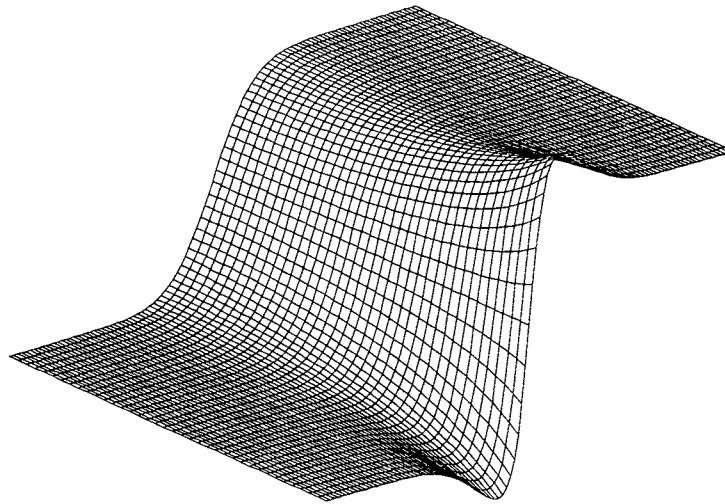


FIG. 6.2. The displacement (with microstructure) as a function of x and t .

a much shorter time-scale and do not even require multiple scale analysis to detect them. The instability of these perturbations into the post-critical region indicates that the material will move rapidly away from the region in which $g'(\gamma) < 0$ to the flat part of the $\gamma - T$ curve (cf. Fig. 3.1).

Numerical approximations will be required in order to investigate larger perturbations to the critical state and more general stress states. The results in this paper will be useful in the interpretation of the numerical experiments. Similar analyses (to those performed in this paper) of the discretized equations can be used to determine if observed phenomena in the numerical results are due to the physical model or if they

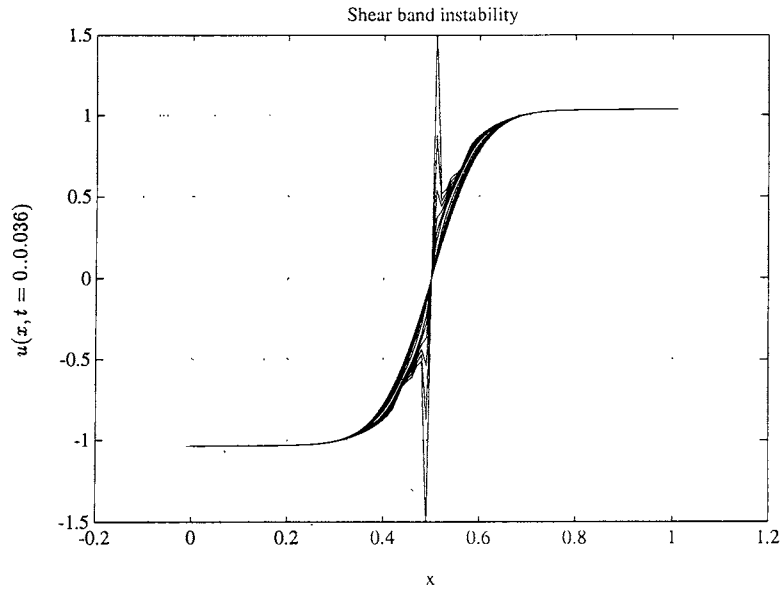


FIG. 6.3. The displacement (without microstructure) which is shown at different time-steps.

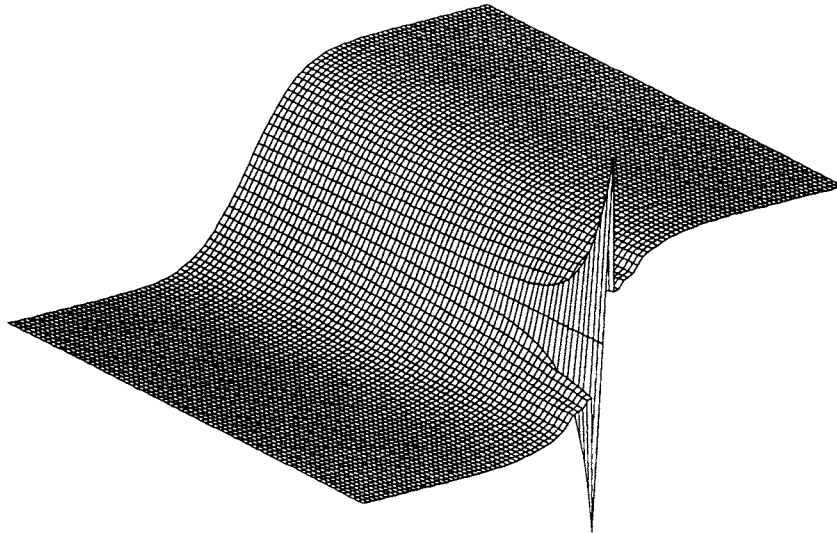


FIG. 6.4. The displacement (without microstructure) as a function of x and t .

are artifacts that can be attributed to the discretization process. The analysis carried out in this paper can be generalized to multi-dimensional models in order to examine post-critical behavior.

Acknowledgments. The first author is grateful to Prof. Chadam for his sponsoring this research program at McMaster and his continuing encouragement.

REFERENCES

- [1] M.J. ABLOWITZ AND P.A. CLARKSON, *Solitons, Nonlinear Evolution Equations and Inverse Scattering*, Cambridge Univ. Press, London, 1991.
- [2] LIANJUN AN, *Loss of hyperbolicity in elastic-plastic material at finite strains*, SIAM J. Appl. Math., 53 (1993), pp. 621–654.
- [3] ———, *The genericity of flutter ill-posedness in 3-dimensional elastic-plastic models*, Quart. Appl. Math., 52 (1994), pp. 343–362.
- [4] LIANJUN AN AND A. PEIRCE, *The effect of microstructure on elastic-plastic models*, SIAM J. Appl. Math., 54 (1994), pp. 708–730.
- [5] ———, *Numerical Investigation of the Effect of Microstructure on the Localization of Deformation*, preprint, 1994.
- [6] LIANJUN AN AND D. SCHAEFFER, *The flutter instability in granular flow*, J. Mech. Phys. Solids, 40 (1992), pp. 683–698.
- [7] G.W. BAXTER, R. BEHRINGER, T. FAGER, AND G.A. JOHNSON, *Pattern formation in flowing sand*, Phys. Rev. Letters, 62 (1989), pp. 2825–2828.
- [8] R.K. BRUMMER AND A.J. RORKE, *Mining induced fracturing around deep gold mine stopes*, Research report No. 38/84, Rock Mechanics Laboratory, South Africa.
- [9] P.A. CLARKSON AND M.D. KRUSKAL, *New similarity reductions of the Boussinesq equation*, J. Math. Phys., 30 (1989), pp. 2201–2213.
- [10] R.K. DODD, J.C. EIBECK, J.D. GIBBON, AND H.C. MORRIS, *Solitons and Nonlinear Wave Equations*, Academic Press, London, 1982.
- [11] J. MANDEL, *Condition de stabilité et postulat de Drucker*, in Rheology and Soil Mechanics, J. Kravtchenko and P. Sirieys, eds., IUTAM symposium at Grenoble, Springer-Verlag, New York, 1966, pp. 58–68.
- [12] J. RICE, *The localization of plastic deformation*, in Proc. 14th IUTAM congress, W. Koiter, ed., Delft, the Netherlands, 1976, pp. 207–220.
- [13] D. SCHAEFFER, *Instability and ill-posedness in the deformation of granular materials*, Intl. J. Num. Anal. Mech. Geomech., 14 (1990), pp. 253–278.
- [14] ———, *A mathematical model for localization in granular flow*, Proc. Roy. Soc. London A, 436 (1992), pp. 217–250.
- [15] J. SMOLLER, *Shock Waves and Reaction-Diffusion Equations*, Springer-Verlag, New York, 1983.
- [16] G.B. WHITHAM, *Linear and Nonlinear Waves*, John Wiley & Sons, Inc., New York, 1974.